

Synthesis and structure of $\text{Fe}_4(\text{CO})_{10}(\mu_2\text{-CO})(\mu_4\text{-Te})_2$ and ^{57}Fe Mössbauer spectra of $\text{Fe}_3(\text{CO})_9(\mu_3\text{-Te})_2$ and $\text{Fe}_4(\text{CO})_{10}(\mu_2\text{-CO})(\mu_4\text{-Te})_2$

Thomas F. Fässler ^{a,*}, Thomas Vögl ^a, Pavel B. Fabritchnyi ^{1,b}, Mikhail I. Afanasov ^b

^a *Laboratorium für Anorganische Chemie, ETH Zurich, Universitätstr. 6, CH-8092 Zurich, Switzerland*

^b *Department of Chemistry, M.V. Lomonosov Moscow State University, 119899 Moscow, Russian Federation*

Received 16 February 1998

Abstract

The compound $\text{Fe}_4(\text{CO})_{10}(\mu_2\text{-CO})(\mu_4\text{-Te})_2$ (**1**) has been prepared by the reaction of $\text{Fe}_3(\text{CO})_9\text{Te}_2$ (**2**) and $\text{Fe}_2(\text{CO})_9$ in toluene. Compound **1** is also formed by UV light irradiation of **2** and $\text{Fe}(\text{CO})_5$ in THF. The structure of **1** was established by single-crystal analysis. Crystal data: orthorhombic, *Pccn*, $a = 6.843(1)$, $b = 15.814(1)$, $c = 17.436(1)$ Å; $V = 1887$ Å³; $Z = 4$; $T = 293$ K, $R_1 = 0.040$. **1** consists of a planar array of four iron atoms with a quadruply bridging telluro ligand on each side of the plane. The shortest metal–metal bond contains a bridging carbonyl ligand, semi-bridging carbonyl ligands bridge the two adjacent metal–metal bonds. ¹²⁵Te-NMR investigations show a conversion from **1** to **2** within several hours. ⁵⁷Fe Mössbauer spectra show two doublets for **1** and only one broadened doublet for **2**. The ratio of the intensities of the doublets of **1** is found close to unity and confirms the existence of two equipopulated crystallographic sites of iron. On the contrary, in the case of **2**, the analysis of the spectra does not allow the expected correlation with the results of the crystal structure determination. The same difficulty was previously encountered in the case of the isostructural selenide $\text{Fe}_3(\text{CO})_9\text{Se}_2$. © 1998 Elsevier Science S.A. All rights reserved.

Keywords: Iron; Tellurium; Mössbauer spectroscopy

1. Introduction

The use of single atom bridges for the stabilization of metal–metal bonds is well established for trigonal-bipyramidal $\text{M}_3(\text{CO})_9(\mu_3\text{-X})_2$ (**A**) and square-bipyramidal $\text{M}_4(\text{CO})_{10}(\mu_2\text{-CO})(\mu_4\text{-X})_2$ (**B**) clusters, where $\text{M} = \text{Fe}$, Ru and Os and the ligands X are elements of group 16 [1]. In both cluster types, the main group elements bridge a metal framework consisting of a distorted triangle with two and a distorted square with four bonding metal–metal distances, respectively (Fig. 1). Wade's electron counting rules describe clusters **A** and **B** as *nido*- and *closo*-clusters, respectively [2].

Several chalcogen-containing clusters consisting of one kind of metal or two different metals have been

structurally characterized: $\text{Fe}_3(\text{CO})_9(\mu_3\text{-X})(\mu_3\text{-Y})$ ($\text{X}, \text{Y} = \text{S}, \text{Se}, \text{Te}$) [3]; $\text{Os}_3(\text{CO})_9(\mu_3\text{-X})_2$ ($\text{X} = \text{S}$ [4]a, Se [4]b) with structure **A** and $\text{Fe}_4(\text{CO})_{10}(\mu_2\text{-CO})(\mu_4\text{-X})_2$ ($\text{X} = \text{S}$ [5], Se [6]); $\text{Fe}_3\text{Ru}(\text{CO})_{10}(\mu_2\text{-CO})(\mu_4\text{-Se})_2$ [6]; $\text{Fe}_2\text{Ru}_2(\text{CO})_{10}(\mu_2\text{-CO})(\mu_4\text{-Te})_2$ [7]; $\text{Ru}_4(\text{CO})_{10}(\mu_2\text{-CO})(\mu_4\text{-X})_2$ [8].

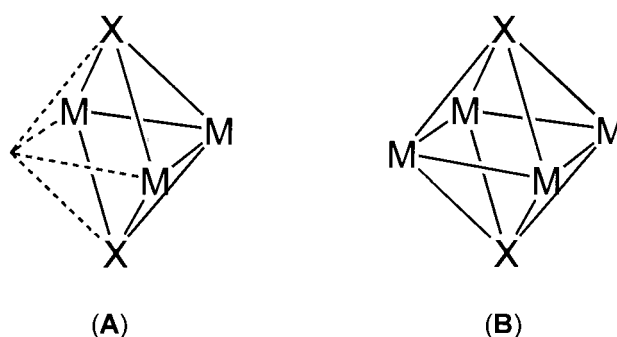


Fig. 1. Central cluster unit in $\text{M}_3(\text{CO})_9(\mu_3\text{-X})_2$ (**A**) and $\text{M}_4(\text{CO})_{10}(\mu_2\text{-CO})(\mu_4\text{-X})_2$ (**B**).

* Corresponding author. Fax: +41 1 6321149; e-mail: faessler@inorg.chem.ethz.ch

¹ E-mail: pf@mstrm.chem.msu.su

$\text{CO}(\mu_4\text{-X})_2$ (X = Se [8]a, Te [8]b) with structure **B**. All compounds of type **A** and of type **B** are isotypic within each series, having triclinic (space group $P\bar{1}$) and orthorhombic ($Pccn$) symmetry, respectively. In all clusters $\text{Fe}_3(\text{CO})_9\text{X}_2$ and $\text{Fe}_4(\text{CO})_{11}\text{X}_2$ at least two different sites of iron atoms are observed by single crystal X-ray analysis, but only one signal is found in the ^{57}Fe Mössbauer spectrum of $\text{Fe}_3(\text{CO})_9\text{Se}_2$ [9].

Here we report the synthesis and crystal structure of $\text{Fe}_4(\text{CO})_{10}(\mu_2\text{-CO})(\mu_4\text{-Te})_2$ (**1**). Up to now, **1** had been reported to be unstable in solution with a rapid conversion to $\text{Fe}_3(\text{CO})_9(\mu_3\text{-Te})_2$ (**2**) [10]. ^{57}Fe Mössbauer spectra of **1** and **2** are also presented.

2. Experimental

All manipulations were carried out under an atmosphere of pure argon with use of standard Schlenk techniques. Solvents were purified, dried and distilled under argon prior to use. $\text{Fe}_3(\text{CO})_9\text{Te}_2$ [11] and $\text{Fe}_2(\text{CO})_9$ [12] were prepared by established procedures. Photochemical reactions were carried out in a water-cooled double wall Duran glass vessel using a mercury lamp, type Hanau TQ 150. IR spectra were recorded on a Perkin-Elmer 883 spectrometer on solutions in CaF_2 cells.

2.1. Preparation of $\text{Fe}_4(\text{CO})_{10}(\mu_2\text{-CO})(\mu_4\text{-Te})_2$ (**1**)

A mixture of **2** (1.00 g, 1.48 mmol) and $\text{Fe}_2(\text{CO})_9$ (2.15 g, 5.92 mmol) in 50 ml of toluene was stirred for 10 min at 35°C. After removal of the solvent and $\text{Fe}(\text{CO})_5$ in vacuo, the residue was first extracted with hexane (2000 ml) until all unreacted **2** had been removed, further extraction with CH_2Cl_2 (50 ml) gave pure $\text{Fe}_4(\text{CO})_{10}(\mu_2\text{-CO})(\mu_4\text{-Te})_2$ (yield 0.32 g, 27% based on **2**).

The optional use of chromatographic work-up on a silica gel column led only to the isolation of the starting material **2**. UV light irradiation of a THF solution (250 ml) of **2** (200 mg, 0.296 mmol) and $\text{Fe}(\text{CO})_5$ (1 ml, 7.5 mmol) gave only very low yields of **1**. Anal. Calc. (found) for **1**: $\text{C}_{11}\text{Fe}_4\text{O}_{11}\text{Te}_2$ $M = 786.71 \text{ g mol}^{-1}$. C, 16.79 (16.90), Fe 28.40 (28.11), Te 32.44 (31.64).

2.2. Crystal structure determination

A plate-like, black crystal of approximate dimension $0.32 \times 0.16 \times 0.02 \text{ mm}^3$ was used for data collection. All data were collected on a STOE IPDS diffractometer with Mo- K_α -irradiation and an imaging plate system. Data collection at a crystal-to-imaging plate distance of 60 mm ($5.02^\circ < \Theta < 56.14^\circ$) using 90 images over a φ range from 0° to 135° with $\Delta\varphi = 1.5^\circ$ and an irradiation

Table 1
Crystallographic data for $\text{Fe}_4(\text{CO})_{10}(\mu_2\text{-CO})(\mu_4\text{-Te})_2$ (**1**)

Chemical formula	$\text{C}_{11}\text{Fe}_4\text{O}_{11}\text{Te}_2$
Formula weight (g mol^{-1})	786.71
Temperature (K)	298
Wavelength, λ , Mo- K_α (\AA)	0.71073
Space group	$Pccn$ (No. 56)
a (\AA)	6.843(1)
b (\AA)	15.814(1)
c (\AA)	17.436(1)
V (\AA^3)	1887(2)
Z	4
$\rho_{\text{calc.}}$ (g cm^{-3})	2.769
μ (cm^{-1})	60.97
R	0.040 ^a
R_w	0.103 ^a

^a $R_1 = \Sigma(F_o - F_c)/\Sigma F_o$, $R_w = [\Sigma w(F_o^2 - F_c^2)]^{1/2}/[\Sigma wF_o^4]^{1/2}$, $w = 1/(\sigma^2(F_o^2) + (0.0485P)^2 + 9.8835P)$, $P = F_o^2 + 2F_c^2/3$.

time of 20 min gave a total of 11094 reflections, of which 2293 were unique ($R_{\text{int.}}$ 0.069%). Structure solution and refinement was undertaken with the SHELXS and SHELXL-93 packages [13] using direct methods and full-matrix least-square routines, respectively. The refinement (based on F^2) was carried out using 1826 reflections with $I > 2\sigma(I)$ and 129 parameters. Data were corrected for Lorentz and polarization effects. Further crystallographic data, final atomic coordinates and selected bond distances and angles are given in Tables 1–3, respectively. Further details of the crystal structure of **1** may be requested from the Fachinformationszentrum Karlsruhe, Gesellschaft für wissenschaftliche Information mbH, D-76344 Eggenstein-Leopoldshafen 2, Germany, on quoting the depository number CSD-101515, the names of the authors and the journal citation.

Table 2
Unit cell parameters and selected distances (\AA) for $\text{Fe}_4(\text{CO})_{10}(\mu_2\text{-CO})(\mu_4\text{-X})_2$

X	S [5]	Se [6]	Te, 1
a	6.603(1)	6.655(1)	6.843(1)
b	15.429(3)	15.587(2)	15.814(1)
c	17.292(4)	17.387(2)	17.436(1)
Fe(1)–Fe(1a)	2.605(2)	2.689(2)	2.838(1)
Fe(1)–Fe(2)	2.532(2)	2.569(1)	2.693(1)
Fe(2)–Fe(2)	2.489(3)	2.534(1)	2.564(2)
X(1)–Fe(1)	2.294(2)	2.406(1)	2.5588(9)
X(1)–Fe(1a)	2.278(2)	2.398(1)	2.553(1)
X(1)–Fe(2)	2.332(2)	2.449(1)	2.610(1)
X(1)–Fe(2a)	2.347(2)	2.458(1)	2.608(1)
Fe– $\text{C}_{\text{CO-terminal}}$ ^a	1.77(1)	1.790(6)	1.788(8)
Fe– $\text{C}_{\text{CO-semibridging}}$	1.79(1)	1.807(6)	1.789(8)
	—	2.418(6)	2.499(8)
Fe– $\text{C}_{\text{CO-bridging}}$	1.93(1)	1.950(6)	1.951(8)

^a Mean values.

Table 3
Selected bond angles of **1** (°)

Te(1a)–Fe(1)–Te(1)	85.65(3)	Fe(2a)–Fe(2)–Fe(1)	92.91(2)
Te(1a)–Fe(1)–Fe(2)	59.56(3)	Te(1)–Fe(2)–Fe(1)	57.55(3)
Te(1)–Fe(1)–Fe(2)	59.53(3)	Te(1a)–Fe(2)–Fe(1)	57.55(3)
Te(1a)–Fe(1)–Fe(1a)	56.38(3)	Fe(1a)–Te(1)–Fe(1)	67.35(3)
Te(1)–Fe(1)–Fe(1a)	56.17(4)	Fe(1a)–Te(1)–Fe(2)	95.06(3)
Fe(2)–Fe(1)–Fe(1a)	87.09(2)	Fe(1)–Te(1)–Fe(2)	62.90(3)
Fe(2a)–Fe(2)–Te(1)	60.59(3)	Fe(1a)–Te(1)–Fe(2a)	62.80(3)
Fe(2a)–Fe(2)–Te(1a)	60.54(3)	Fe(1)–Te(1)–Fe(2a)	95.18(3)
Te(1)–Fe(2)–Te(1a)	83.50(3)	Fe(2)–Te(1)–Fe(2a)	58.86(4)

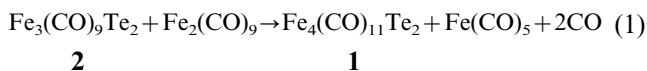
2.3. ^{125}Te -NMR spectroscopy and Mössbauer spectra

The spectra were recorded on a Bruker 300 MHz-spectrometer at 111.92 MHz. The chemical shift convention used is a negative shift for a chemical shift to higher field of the reference compound $\text{Te}(\text{Me})_2$.

Mössbauer spectra were recorded using a conventional spectrometer of the electrodynamic type operating in the constant acceleration mode, which was calibrated against metallic iron foil. Mössbauer parameters were calculated from the least-squares fit to a Lorentzian line shape. The sources used for ^{57}Fe Mossbauer-effect experiments were $^{57}\text{Co}/\text{Cu}$ or $^{57}\text{Co}/\text{Rh}$, either being kept at r.t. during the measurement. All isomer shifts of ^{57}Fe are reported with respect to a spectrum of α -Fe at 295 K. The source used for ^{125}Te measurements ($^{125}\text{Sb}/\text{Cu}$) was cooled to 80 K.

3. Synthetic and crystallographic results

Stirring of **2** with $\text{Fe}_2(\text{CO})_9$ in a toluene solution at 35°C for 10 min formed the tetranuclear cluster **1** in moderate yields (Eq. (1)). We found that compound **1** is also formed, in lower yield, by UV light irradiation of **2** and $\text{Fe}(\text{CO})_5$ in THF. The IR spectrum of **1** in the carbonyl region shows bands (in CH_2Cl_2) at 2072 (w), 2026 (s), 2010 (m, sh), 2000 (w, sh), 1983 (m) and 1821 (w) cm^{-1} . The pattern and the presence of both terminal and bridging carbonyl groups indicate the structural similarity to $\text{M}_4(\text{CO})_{10}(\mu_2\text{-CO})(\mu_4\text{-X})_2$ [5,7,8,10,14].



The ^{125}Te -NMR spectrum in CD_2Cl_2 shows one signal at 572 ppm shifted to higher field from **2** which shows a signal at 1056 ppm in C_6D_6 ([3]c) and at 1124 in CD_2Cl_2 . After several hours a second signal at 1124 ppm is observed indicating decomposition and formation of **2**.

Single crystals of **1** suitable for single crystal X-ray analysis were obtained from a CH_2Cl_2 solution at -20°C . The molecular structure of **1** is shown in Fig.

2. The cluster consists of a planar arrangement of four iron atoms with quadruply bridging tellurium atoms on each side of the Fe_4 unit. One edge of the metal unit is symmetrically bridged by a carbonyl group, giving rise to a short iron–iron contact of the Fe_4 -unit ($\text{Fe}(2)–\text{Fe}(2a)$ 2.564(2) Å). The opposite edge of the distorted metal square occurs with the longest iron–iron contact ($\text{Fe}(1)–\text{Fe}(1a)$ 2.838(1) Å). The two other sides are bridged by semi-bridging carbonyls with longer contacts to $\text{Fe}(2)$ ($\text{Fe}(2)–\text{C}(5)$ 2.499(8) Å) and shorter ones to $\text{Fe}(1)$ ($\text{Fe}(1)–\text{C}(5)$ 1.789(8) Å). The iron atoms which are linked via the semi-bridging carbonyl groups show an intermediate distance ($\text{Fe}(1)–\text{Fe}(2)$ 2.693(1) Å) compared with the other metal–metal bonds.

The crystallographic twofold axis runs through the bridging carbonyl group C(3), O(3) bisecting the two iron–iron connections $\text{Fe}(2)–\text{Fe}(2a)$ and $\text{Fe}(1)–\text{Fe}(1a)$ at the midpoints. The molecule has approximate C_{2v} symmetry with two (non-crystallographic) mirror planes, one coplanar with the two tellurium atoms and the symmetrically bridging carbonyl group (C(3), O(3)) and one through the four iron atoms and all bridging carbonyl groups. As indicated by the space group and the cell parameters, the structure of **1** is isotopic to that of $\text{Fe}_4(\text{CO})_{11}\text{S}_2$ [5] and $\text{Fe}_4(\text{CO})_{11}\text{Se}_2$ [6]. Cell parameters and all intramolecular distances of the distorted octahedral clusters $\text{Fe}_4(\text{CO})_{11}\text{X}_2$ (X = S, Se, Te) increase from sulfur to tellurium (Table 2). This corresponds to increasing atomic radii of the X atoms. All compounds of the type $\text{Fe}_4(\text{CO})_{11}\text{X}_2$ have longer X–Fe(2) contacts than X–Fe(1) probably due to the influence of the carbonyl group bridging the $\text{Fe}(2)–\text{Fe}(2)$ edge.

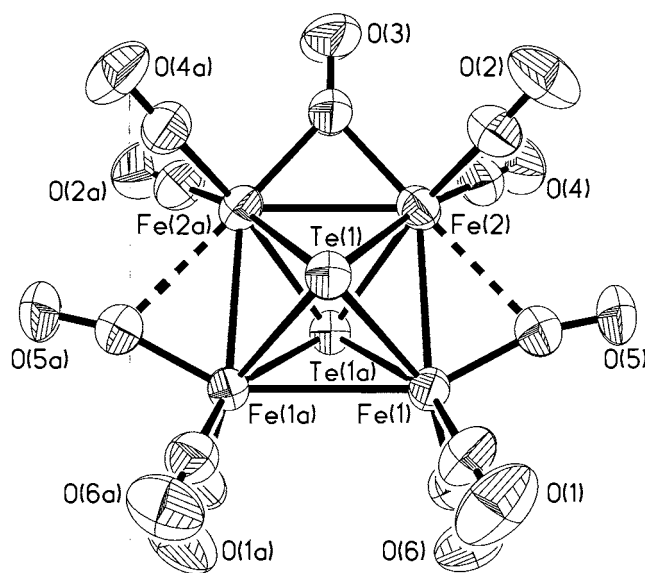


Fig. 2. Molecular structure of $\text{Fe}_4(\text{CO})_{10}(\mu_2\text{-CO})(\mu_4\text{-Te})_2$ (**1**) with ellipsoids at 50% probability level.

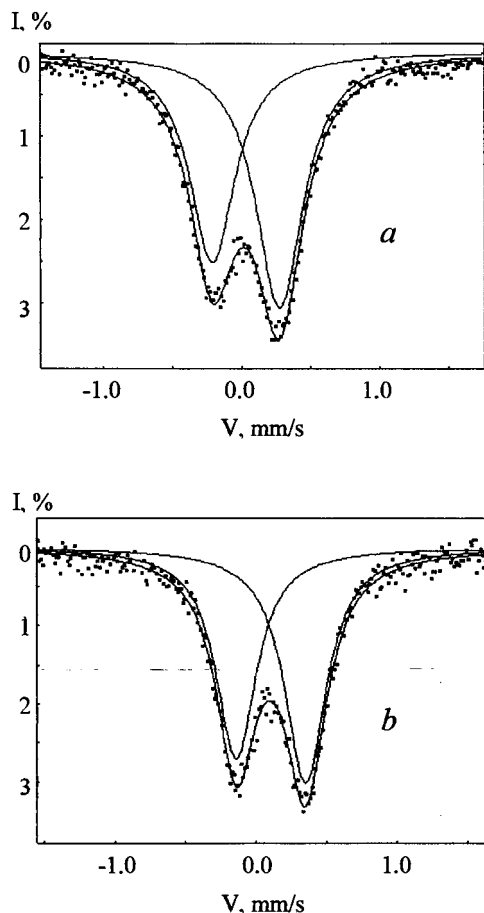


Fig. 3. ^{57}Fe Mössbauer spectra of **2** recorded at 295K (a) and 80 K (b).

4. Mössbauer spectra

^{57}Fe Mössbauer spectra of $\text{Fe}_3(\text{CO})_9\text{Te}_2$ (**2**), recorded at 295 and 80 K (Fig. 3(a) and (b)), consist of a broadened asymmetric doublet (isomer shift $\delta = 0.03 \pm 0.01 \text{ mm s}^{-1}$, quadrupole splitting $\Delta = 0.48 \pm 0.02 \text{ mm s}^{-1}$, full width at half maximum for each component $\Gamma = 0.34 \pm 0.02 \text{ mm s}^{-1}$ at 295 K; $\delta = 0.10 \pm 0.01 \text{ mm s}^{-1}$, $\Delta = 0.50 \pm 0.02 \text{ mm s}^{-1}$, $\Gamma = 0.35 \pm 0.02 \text{ mm s}^{-1}$ at 80 K). On the basis of the crystal structure of this compound it seems reasonable to interpret the observed broadening as a result of superposition of two doublet contributions reflecting the presence of two crystallographically different iron sites. However, such a hypothesis appears to be in contradiction with the results of a closer examination of the spectra. In fact, if we accordingly assume a model of two doublets with narrow components (imposing $\Gamma = 0.27 \text{ mm s}^{-1}$, which is the value observed for a standard sodium nitroprusside absorber) the fitting model leads to two doublets having the same areas A . Such a result is obviously inconsistent with the expected proportion $\text{Fe}(1):\text{Fe}(2) = 2:1$ and cannot be imputed to different values of recoil-free fraction (f -factor) for the two sites because the ratio of the areas is virtually the same at

295 and 80 K. Hence, this discrepancy shows that the simplest model does not allow an explanation of spectra of **2**. Their broadening points towards a distribution of hyperfine parameters that are unrelated to the crystallographic sites (and as is also the case in the other compound reported here). Interestingly, a single doublet spectrum was also observed by Kalvius et al. [9] for the isostructural selenide $\text{Fe}_3(\text{CO})_9\text{Se}_2$. The reported values of δ and Δ agree well with those we obtained (cp. spectrum in Fig. 3(a), i.e. $\delta = 0.03 \text{ mm s}^{-1}$, $\Delta = 0.48 \text{ mm s}^{-1}$, the Γ value was not specified for the selenide complex). It shows that hyperfine interactions of ^{57}Fe in both chalcogenides are not noticeably affected by different chalcogen atoms.

The spectrum of $\text{Fe}_4(\text{CO})_{11}\text{Te}_2$ (**1**) recorded at 295 K (Fig. 4(a)) is very different from that of $\text{Fe}_3(\text{CO})_9\text{Te}_2$. Here computer analyses reveal the presence of two symmetric doublets with the following parameters: doublet I: $\delta(\text{I}) = 0.00 \pm 0.01 \text{ mm s}^{-1}$, $\Delta(\text{I}) = 0.71 \pm 0.02 \text{ mm s}^{-1}$, $\Gamma(\text{I}) = 0.31 \pm 0.01 \text{ mm s}^{-1}$, $A(\text{I}) = 57 \pm 1\%$; doublet II: $\delta(\text{II}) = 0.11 \pm 0.01 \text{ mm s}^{-1}$, $\Delta(\text{II}) = 1.04 \pm 0.02 \text{ mm s}^{-1}$, $\Gamma(\text{II}) = 0.31 \pm 0.01 \text{ mm s}^{-1}$, $A(\text{II}) = 43 \pm 1\%$. In contrast to compound **2**, this spectrum unambiguously demonstrates the structural non equivalence of two iron sites [15].

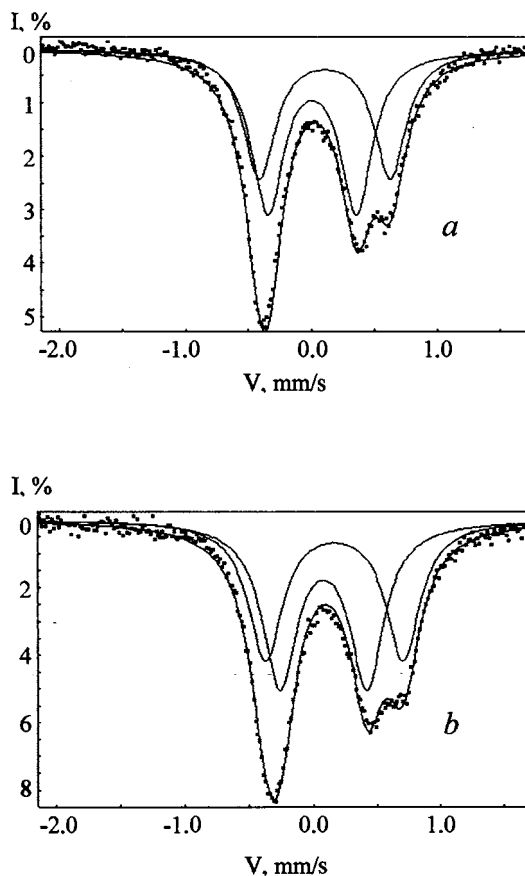


Fig. 4. ^{57}Fe Mössbauer spectra of **1** recorded at 295K (a) and 80 K (b).

The observation of unequal values of $A(I)$ and $A(II)$ is only apparently inconsistent with the expected ratio $Fe(1):Fe(2) = 1:1$ and suggest a lower r.t. value of the recoil-free fraction for the iron associated with doublet II. A $A(I)/A(II)$ value, which is significantly closer to the anticipated one, is actually recovered in the spectrum recorded at lower temperature (Fig. 4b), i.e. under conditions attenuating differences in thermal vibration amplitudes. The low-temperature Mössbauer parameters of the two doublets (doublet (I): $\delta(I) = 0.08 \pm 0.01$ mm s⁻¹, $\Delta(I) = 0.68 \pm 0.01$ mm s⁻¹, $\Gamma(I) = 0.32 \pm 0.01$ mm s⁻¹, $A(I) = 53 \pm 1\%$; doublet (II): $\delta(II) = 0.17 \pm 0.01$ mm s⁻¹, $\Delta(II) = 1.08 \pm 0.01$ mm s⁻¹, $\Gamma(II) = 0.32 \pm 0.01$ mm s⁻¹, $A(II) = 47 \pm 1\%$) show no sensible variation within experimental error for both $\Delta(I)$ and $\Delta(II)$, whereas the observed slight increase in δ values is in agreement with the expected evolution of the second order Doppler shift on lowering the temperature. Comparison with the Mössbauer parameters of these two spectral components leads therefore, to the conclusion that the iron atoms accountable for the doublet II are characterized by lower values of the electronic charge density at the nucleus ($\delta(II) > \delta(I)$), higher values of the electric field gradient ($\Delta(II) > \Delta(I)$) and greater mean-square amplitudes of the thermal vibration ($A(II) < A(I)$).

5. Discussion

In contrast to an earlier report, a synthetic route to **1** was developed. ¹²⁵Te-NMR investigation show a conversion from **1** to **2** within several hours. The presence of the same number of Fe(1) and Fe(2) atoms in **1** does not allow a clear assignment to the ⁵⁷Fe Mössbauer spectra based on the analysis of the relative intensities of the observed spectral components. On the other hand, any assignment based exclusively on interpreting the differences found for the two sets of Mössbauer parameters seems also rather doubtful due to complex bonding interactions of both Fe(1) and Fe(2) atoms with various neighboring atoms. However, on considering Fig. 2, it can be assumed that the mentioned differences reflect primarily the presence of bridging carbonyl groups, which are only present in the coordination sphere of Fe(2). The Fe(2) atoms, which are linked via this bridging carbonyl ligand, have the shortest iron–iron contact and slightly larger equivalent displacement components if compared with those of Fe(1). So we tempt to ascribe the doublet II ($A(I) > A(II)$) to the Fe(2) site. A tendency of larger displacement vectors of Fe(2) is also found in other compounds which are isotypic of **1** ([6], [8]b). Comparing the values of $\Delta(I)$ and $\Delta(II)$ with those of compound Fe₃(CO)₉Te₂ **2** ($\Delta = 0.48 \pm 0.02$ mm s⁻¹), a much smaller difference appears between $\Delta(I)$ and Δ . This is consistent with the

fact that in compound **1** the Fe(1) atoms, which had been assigned with doublet I, are bonded to three terminal (semi-bridging) carbonyl groups as all iron atoms are in **2**. Further investigations are obviously needed for the interpretation of the features of the electronic state of the different iron atoms of **2**. In this context, it should be noted that we did not observe any perceptible resonance absorption in ¹²⁵Te Mössbauer experiments at 80 K for **1** and **2**, which indicates very small recoil-free fractions associated with the 35.6 keV transition for tellurium in these cluster compounds.

Acknowledgements

This work was funded by a grant from the Swiss National Science Foundation. We are grateful to Professor R. Nesper, ETH Zürich, for his generous support and to Professor J. Rouxel, Institut des Materiaux de Nantes, for the interest in this work.

References

- [1] (a) K.H. Whitmire, J. Coord. Chem. 17 (1988) 17. (b) G. Huttner, K. Knoll, Angew. Chem. Int. Ed. Engl. 26 (1987) 743. (c) H. Vahrenkamp, Adv. Organomet. Chem. 22 (1983) 169.
- [2] K. Wade, Adv. Inorg. Chem. Radiochem. 18 (1976) 1.
- [3] (a) C.H. Wei, L.F. Dahl, Inorg. Chem. 4 (1965) 493. (b) P. Hubener, E. Weiss, Cryst. Struct. Commun. 11 (1982) 331. (c) L.F. Dahl, P.W. Sutton, Inorg. Chem. 2 (1963) 1067. (d) H. Schumann, M. Magerstadt, J.J. Pickart, Organomet. Chem. 240 (1982) 407. (e) G. Gervasio, J. Organomet. Chem. 445 (1993) 147.
- [4] (a) R.D. Adams, I.T. Horvath, B. Segmüller, L. Yang, Organometallics 2 (1983) 144. (b) B.F.G. Johnson, J. Lewis, P.G. Lodge, R.R. Raithby, Acta Crystallogr. 37B (1981) 173.
- [5] R.D. Adams, J.E. Babin, J. Estrada, J.-G. Wang, Polyhedron 8 (1989) 1885.
- [6] P. Mathur, Md.M. Hossain, R.S. Rashid, J. Organomet. Chem. 467 (1994) 245.
- [7] P. Mathur, I.J. Mavankal, V. Rugmini, M.F. Mahon, Inorg. Chem. 29 (1990) 4838.
- [8] (a) B.F.G. Johnson, T.M. Layer, J. Lewis, A. Martin, R.R. Raithby, J. Organomet. Chem. 429 (1992) C41. (b) P. Mathur, B.H.S. Thimmappa, A.L. Rheingold, Inorg. Chem. 29 (1990) 4658.
- [9] M. Kalvius, W. Wiedmann, U. Zahn, P. Kienle, Bull. Am. Phys. Soc. 9 (1964) 634.
- [10] P. Mathur, Md.M. Hossain, R.S. Rashid, J. Organomet. Chem. 460 (1993) 83.
- [11] W. Hieber, J. Gruber, Z. Anorg. Allg. Chem. 296 (1958) 91.
- [12] E.H. Braye, W. Hubel, Inorg. Chem. 8 (1966) 178.
- [13] SHELXS-86, SHELXL-93, G.M. Sheldrick, University of Göttingen, BRD.
- [14] P. Mathur, D. Chakrabarty, Md.M. Hossain, R.S. Rashid, J. Organomet. Chem. 420 (1991) 79.
- [15] The broadening, occurring in this compound also affects to the same extent both doublets attributable to crystallographically different iron sites. This indicates a similar distribution of ⁵⁷Fe hyperfine parameters for both sites. Such a 'non-intrinsic' distribution, already encountered in the case of **2**, probably arises from an insufficient crystallinity of the samples used in Mössbauer measurements.